Generalized SINR Analysis for Device-to-Device Communications

Imène Trigui*, Ben Liang*, and Sofiène Affes†
*University of Toronto 10 King's College Road Toronto, Ontario M5S 3G4, Canada.
†INRS-EMT, 800, de la Gauchetiere Ouest, Bureau 6900, Montreal, H5A 1K6, Qc, Canada

***Abstract*—This paper provides an analytically tractable framework for investigating a fading model-free statistical distribution of the signal-to-interference-plus-noise power ratio (SINR) in Poison distributed cellular networks subject to device-to-device (D2D) transmissions. Our main finding show that a closed-form SINR distribution may be obtained for any fading scenario in which the per-link power gain follows the product of two Fox's H-function probability density function thereby subsuming most of the coverage probability expressions previously presented for all the known simple and composite fading models.**

***Index Terms*—Device-to-device, stochastic geometry, coverage probability, Fox's-H function.**

I. INTRODUCTION

Computing the SINR distribution in Poison distributed cellular networks is significantly tractable only for fading channels and transmission schemes whose equivalent per-link power gains follow a Gamma distribution with integer shape parameter ([1], [2] and references therein). Such particular fading distributions, by leading to exponential expressions for the conditional SINR that enable averaging via the Laplace transform of the interference, have very often limited legitimacy according to [3], [4], who argued that these fading models may fail to capture new and more realistic fading environments. This is particularly true as new communication technologies accommodating a wide range of usage scenarios with diverse link requirements are continuously being introduced and analyzed, for example, device-to-device and body-centric communications, free-space optical (FSO) communications, and millimeter-wave communications. In fact, the design of such new communication paradigms need to acquire flexibility to account for disparate signal propagation mechanisms.

Over the past few years, several new fading models have been introduced to model either the fading or the joint fading/shadowing phenomena. These models, including the κ-μ [3], the shadowed κ-μ [5], the Weibull [6] and the generalized $\mathcal{K}$ [7], among many others, generally offer a better fit to the fading observed in a range of real-world applications than the classical Rayleigh, Nakagami-m, and Rician distributions.

Some prior works have already made a good progress on the analysis of the distribution of the SINR by presuming a specific channel gain model [8]- [9]. However, besides being channel-model dependent, they relied on series representation methods (e.g., infinite series in [10] and Laguerre polynomial series in [9]) thereby expressing the interference functionals as an infinite series of higher order derivative terms given by the Laplace transform of the interference power. These methods cannot lend themselves to closed-form expressions and hence require complex numerical evaluation.

These aforementioned challenges foster our motive to develop a unified SINR analysis framework that subsumes most, if not all, of the linear and non-linear fading models adopted in the open literature. The general setting of the paper considers single-tier device-to-device (D2D)-enabled cellular network where the D2D links are allowed to share the uplink cellular spectrum. Currently being touted as a potential ingredient of 5th-generation wireless networks, D2D allows direct communication between cellular mobiles, thus bypassing the base stations ([1], [9] and references therein). D2D opens up new opportunities for proximity-based commercial services and particularly social networking applications.

The first main contribution of this paper is to introduce a novel approach to deriving a model-free general expression for the D2D and cellular SINR complementary cumulative density function (CCDF). Due to the generality of the CCDF and Laplace transform of the interference power, they have been successfully applied to arbitrary Nakagami-m, the Weibull, the generalized $\mathcal{K}$, and shadowed κ-μ fading models. This paper, further embody the Fox's H-transform theory, wherein integral transforms involve Fox's H-functions as kernels, for modeling and analysis of D2D enabled cellular network, which is in fact new.

II. SYSTEM MODEL

Consider a set of macro-cellular BSs and a set of D2D users operating in the uplink through an overlaid spectrum access. The overlaid spectrum access scheme allocates orthogonal time/frequency resources to the cellular and D2D transmitters by dividing the uplink spectrum into two non-overlapping portions. The locations of macro-cellular BSs and D2D users are modeled as independent homogeneous Poisson point processes

978-1-5386-3531-5/17/$31.00 © 2017 IEEE

(PPP) Ψ_c and Ψ_d with intensities λ_c and λ_d, respectively.

In this setting, the received power at the typical receiver located at the origin can be written as

$$P_x^r = P_{0,x} h_{0,x} L_{0,x}^{-\alpha}, \quad x \in \{c, d\} \tag{1}$$

where $P_{0,x}$, $h_{0,x}$ and $L_{0,x}$ are the power of the typical transmitter, the fading power in the typical transceiver channel, and the distance between the typical transmitter and receiver, respectively, and $\alpha > 2$ is the path-loss exponent. Let the Point Processes (PP) $\widetilde{\Psi}_c \subset \Psi_c$ and $\widetilde{\Psi}_d \subset \Psi_d$ denote the set of interfering cellular UEs with intensity λ_c and the set of interfering D2D UEs with intensity $\tau\lambda_d$, respectively, where $0 \leq \tau \leq 1$ is the ALOHA transmit probability on each time slot. Then, the D2D and cellular interference at the typical receiver are

$$I_d = \sum_{i \in \widetilde{\Psi}_d \setminus \{0\}} P_{i,d} h_{i,d} L_{i,d}^{-\alpha} \tag{2}$$

$$I_c = \sum_{i \in \widetilde{\Psi}_c} P_{i,c} h_{i,c} L_{i,c}^{-\alpha} \tag{3}$$

where P_i , h_i, and L_i, denote the transmit power, the fading power, and the locations of macro-cellular UEs (subscript c) and D2D users (subscript d). In this paper, we use channel inversion for power control, i.e., $P_i = L_i^{\alpha}$.

III. Generalized SINR Analysis

Theorem 1: With overlay in-band D2D, the SINR complementary cumulative distribution function (CCDF) of D2D and cellular links, defined as $\mathbb{P}^x(T) \triangleq \mathbb{P}\left(\mathrm{SINR}_x = \frac{P_x^r}{I_x + \sigma^2} \geq T\right)$ for $x \in \{d, c\}$, is given by

$$\begin{aligned}\mathbb{P}^x(T) &= \frac{1}{T}\int_0^{\infty} \mathcal{E}_h\left[h\ \mathrm{G}_{1,2}^{1,0}\left[\frac{h\xi}{T}\,\middle|\,\begin{matrix}0\\0,-1\end{matrix}\right]\right] \\ &\quad\times \exp\!\left(-\xi\sigma^2 - \mathcal{A}^x(\xi,\delta)\right) d\xi,\end{aligned} \tag{4}$$

where $\mathcal{E}_z[.]$ is the expectation with respect to the random variable z, $\mathrm{G}_{a,b}^{c,d}[\cdot]$ denotes the Meijer's-G function [12, Eq. 9.301] and

$$\begin{cases}\mathcal{A}^d(\xi,\delta) = \pi\tau\lambda_d\xi^{\delta}\Gamma\left(1-\delta\right)\mathcal{E}\left[P_d^{\delta}\right]\mathcal{E}\left[h^{\delta}\right], & \text{D2D;}\\ \mathcal{A}^c(\xi,\delta) = \frac{\delta\xi\ \mathcal{E}_{h,P_c}\left[hP_c\ {}_2\mathrm{F}_2\left(1-\delta,1;2-\delta,2;-\frac{\xi P_c h}{R^{2/\delta}}\right)\right]}{R^{2/\delta}(1-\delta)}, & \text{Cellular.}\end{cases} \tag{5}$$

whereby $\delta = \frac{2}{\alpha}$, $P_x = L_x^{\alpha}$ for $x \in \{d, c\}$, and ${}_\mathrm{p}\mathrm{F}_\mathrm{q}(\cdot)$ stands for the generalized hypergeometric function [12, Eq. 9.14.1].

Proof: See Appendix A for details.

Theorem 1 demonstrates the general expressions of the Laplace transforms of I_d and I_c as well as the SINR CCDF without assuming any specific random channel gain and distance models. Notice that, thought in (4) the path loss is fully compensated corresponding to channel inversion, assuming fractional power control (FPC) which partially compensates for path loss, i.e., (i.e., $P_i = L_i^{\epsilon\alpha}$ where $\epsilon \in [0,1]$) is also analytically tractable using [2] and following the same steps as in Appendix A.

Notice that in accordance with [1], the cellular uplink interference Laplace transform is independent of the BS intensity λ_c. While [1] only considers Rayleigh fading, Theorem 1 remarkably extends this invariance property to any fading model.

Hereafter we assume the active cellular transmitter inside the coverage area $\mathcal{U}$ is uniformly distributed in a circular disk $\mathcal{B}(0,R)$ with $\mathbb{P}_{L_c}(x) = 2\pi\lambda_c x\mathbb{I}[x \in [0, 1/\sqrt{\pi\lambda_c}]]$. Moreover, we assume that each potential D2D receiver is randomly and independently placed around its associated potential D2D transmitter with isotropic direction and Rayleigh distributed distance L_d with $\mathbb{P}_{L_d}(x) = 2\pi\zeta x e^{-\pi\zeta x^2}, \quad \zeta > 0$. Accordingly, taking the expectation over $L_x, x \in \{d, c\}$ in (5) yields

$$\begin{cases}\mathcal{A}^d(\xi,\delta) = \frac{\tau\lambda\xi^{\delta}\Gamma(1-\delta)\gamma(2,\zeta\pi\theta^2)}{\zeta}\ \mathcal{E}\left[h^{\delta}\right], & \text{D2D ;}\\ \mathcal{A}^c(\xi,\delta) = \frac{\delta^2\xi\mathcal{E}_h\left[h\,{}_3\mathrm{F}_3(1-\delta,1,1+\delta;2-\delta,2,2+\delta;-\xi h)\right]}{(\delta-1)(\delta+1)}, & \text{Cellular;}\end{cases} \tag{6}$$

where $\mathcal{A}^d(\xi,\nu)$ follows from (5) after recognizing that $\mathcal{E}[P_d^{\delta}] = \mathcal{E}[L_d^2] = \frac{\gamma\left(2,\zeta\pi\theta^2\right)}{\pi\zeta\mathbb{P}(L_d \leq \theta)}$ where θ is a predefined mode selection threshold [1, Eq. 10], and $\gamma(a,z)$ stands for the incomplete Gamma function [12, Eq. 9.100] while letting $\lambda = \lambda_D/\mathbb{P}(L_d \leq \theta)$. In its turn the expectation of $\mathcal{A}^c(\xi,\nu)$ over L_c in (5) follows from applying

$$\begin{aligned}\int z^{\beta-1}{}_2\mathrm{F}_2\left(a_1,a_2;b_1,b_2;cz^r\right)dz &= \\ \frac{z^{\beta}}{\beta}{}_3\mathrm{F}_3\left(\frac{\beta}{r},a_1,a_2;\frac{\beta}{r}+1,b_1,b_2;cz^r\right)&.\end{aligned} \tag{7}$$

Hereafter, let

$$\Phi(\xi,T) = \mathcal{E}_h\!\left[h\ \mathrm{G}_{1,2}^{1,0}\left[\frac{h\xi}{T}\,\middle|\,\begin{matrix}0\\0,-1\end{matrix}\right]\right], \tag{8}$$

then capitalizing on (4) and (6), we would like to emphasize that truly closed-form results may be obtained for any fading scenarios in which the per-link power gain follows the product of two Fox's H-function probability density function [13], [14]. As a case study, hereafter, we focus our attention to Nakagami-m, Weibull, Generalized-$\mathcal{K}$, and shadowed κ-μ fading channels.

Proposition 1 (Nakagami-m Fading): The D2D and cellular links CCDF over Nakagami-m fading is given by

$$\begin{aligned}\mathbb{P}_m^x(T) &= \frac{1}{\Gamma(m)}\int_0^{\infty}\xi^{-1}\mathrm{G}_{2,2}^{1,1}\left[\frac{\Omega\xi}{mT}\,\middle|\,\begin{matrix}1-m,1\\1,0\end{matrix}\right] \\ &\quad\times\exp\left(-\xi\sigma^2 - \mathcal{A}_m^x(\xi,\delta)\right)d\xi,\end{aligned} \tag{9}$$

where

$$\begin{cases}\mathcal{A}_m^d(\xi,\delta) = \frac{\tau\lambda\xi^{\delta}}{\zeta}\left(\frac{\Omega}{m}\right)^{\delta}\frac{\Gamma(1-\delta)\Gamma(m+\delta)\gamma(2,\zeta\pi\theta^2)}{\Gamma(m)},\\ \mathcal{A}_m^c(\xi,\delta) = \frac{\delta^2\xi\Omega\ {}_4\mathrm{F}_3\left(1-\delta,1,1+\delta,m+1;2-\delta,2,2+\delta;-\frac{\Omega\xi}{m}\right)}{(\delta-1)(\delta+1)}.\end{cases} \tag{10}$$

Proof: Let h be a random variable with $f_h(y) = \frac{\left(\frac{m}{\Omega}\right)^m}{\Gamma(m)} x^{m-1} e^{-\frac{m}{\Omega}x}$, then we have

$$\Phi(\xi, T) \overset{(a)}{=} \frac{\Omega}{\Gamma(m+1)} \mathrm{G}_{2,2}^{1,1}\left[\frac{\Omega\xi}{mT}\left|\begin{matrix}-m, 0\\ 0, -1\end{matrix}\right.\right] \tag{11}$$

where (a) follows after using [12, Eq. 7.813]. In the other hand, $\mathcal{A}_m^d(\xi, \nu)$ is obtained from (6) while $\mathcal{E}[h^\delta] = \frac{\Gamma(m+\delta)}{\Gamma(m)}\left(\frac{\Omega}{m}\right)^\delta$ and $\mathcal{A}_m^c(\xi, \nu)$ follows from (6) after applying [12, Eq. 7.522.9]. Plugging all these results in (4) yields $\mathbb{P}_m^x(T)$ after some manipulations. It is worthwhile to mention that $\mathbb{P}_m^x(T)$ is new and constitutes a valuable add on to the existing SINR CCDF analysis frameworks for integer m [15].

Corollary 1: When the D2D communication is interference limited, the SIR CCDF under Nakgami-m fading is given by

$$\mathbb{P}_m^d(T) = \frac{1}{\Gamma(m)} \mathrm{H}_{1,2}^{2,0}\left[\lambda\kappa_m T^\delta \left|\begin{matrix}(1, \delta)\\ (0, 1), (m, \delta)\end{matrix}\right.\right], \tag{12}$$

where $\kappa_m = \frac{\tau\Gamma(1-\delta)\Gamma(m+\delta)\gamma(2,\zeta\pi\theta^2)}{\zeta\Gamma(m)}$ and $H_{p,q}^{m,n}[\cdot]$ is the univariate Fox's-H function [13, Eq.(1.2)].

Proof: In the case of no noise, $\mathbb{P}_m^d(T)$ in (9) becomes

$$\begin{aligned}\mathbb{P}_m^d(T) \quad &\overset{(a)}{=} \quad \frac{1}{\Gamma(m)}\int_0^\infty \xi^{-1}\mathrm{G}_{2,2}^{1,1}\left[\frac{\Omega\xi}{mT}\left|\begin{matrix}1-m, 1\\ 1, 0\end{matrix}\right.\right] \\ &\quad \times \mathrm{H}_{0,1}^{1,0}\left[\mathcal{A}_m^d(\xi, \delta)\left|\begin{matrix}-\\ (0, 1)\end{matrix}\right.\right] d\xi,\end{aligned} \tag{13}$$

where (a) follows after resorting to $\exp(-x) = \mathrm{H}_{0,1}^{1,0}\left[x\left|\begin{matrix}-\\ (0,1)\end{matrix}\right.\right]$. Then, expressing the Meijer-G function in (13) in terms of Fox-H function by means of [13, Eq.(1.111)] and applying [13, Eq.(2.19)] complete the proof.

Proposition 2 (Weibull Fading): The weibull fading channel accounts for the nonlinearity of a propagation medium with a physical fading parameter ν. When h follows a Weibull distribution with parameters $(\nu, \Phi = \Omega^\nu)$ [6], then the SINR CCDF D2D and cellular links is

$$\begin{aligned}\mathbb{P}_{\mathcal{W}}^x(T) = \frac{\nu}{T\Phi}\int_0^\infty \left(\frac{T}{\xi}\right)^{\nu+1} \mathrm{H}_{1,1}^{1,0}\left[\left(\frac{T}{\xi}\right)^\nu \frac{1}{\Phi}\left|\begin{matrix}(1-\nu, \nu)\\ (0, 1)\end{matrix}\right.\right] \\ \times \exp\left(-\xi\sigma^2 - \mathcal{A}_{\mathcal{W}}^x(\xi, \delta)\right) d\xi,\end{aligned} \tag{14}$$

where

$$\begin{cases}\mathcal{A}_{\mathcal{W}}^d(\xi, \delta) = \frac{\tau\lambda\xi^\delta}{\zeta}\Phi^{\frac{\delta}{\nu}}\Gamma\left(1-\delta\right)\Gamma\left(1+\frac{\delta}{\nu}\right)\gamma(2, \zeta\pi\theta^2),\\ \mathcal{A}_{\mathcal{W}}^c(\xi, \delta) = \delta^2 \mathrm{H}_{4,4}^{4,1}\left[\frac{\phi}{\xi}\left|\begin{matrix}(-\nu, 1), (1-\delta, 1), (1, 1), (1+\delta, 1)\\ (1, \frac{1}{\nu}), (\delta, 1), (0, 1), (\delta, 1)\end{matrix}\right.\right].\end{cases} \tag{15}$$

Proof: The proof follows from (8) with $f_h(y) = \frac{\nu}{\Phi}y^{\nu-1}e^{-\frac{y^\nu}{\Phi}} \overset{(a)}{=} \frac{\nu}{\Phi}y^{\nu-1}\mathrm{H}_{0,1}^{1,0}\left[\frac{y^\nu}{\Phi}\left|\begin{matrix}-\\ (0, 1)\end{matrix}\right.\right]$ and applying [13, Eqs. (2.3), (1.56)]. Besides, $\mathcal{A}_{\mathcal{W}}^c(\xi, \nu)$ follows by resorting to $\mathcal{E}[h^\delta] = \Gamma(1+\frac{\delta}{\nu})\phi^{\frac{\delta}{\nu}}$. In the other hand, recalling that ${}_{\mathrm{p}}\mathrm{F}_{\mathrm{q}}(\underline{a}_p; \underline{b}_q; -z) = \mathrm{H}_{p,q+1}^{1,p}\left[z\left|\begin{matrix}(1-\underline{a}_p, 1)\\ (1, 1), (1-\underline{b}_q, 1)\end{matrix}\right.\right]$ and applying [13, Eq. 2.3] yield $\mathcal{A}_{\mathcal{W}}^c(\xi, \nu)$ after some manipulations.

Corollary 2: When the D2D communication is interference limited, the SIR CCDF under Weibull fading is given by

$$\mathbb{P}_{\mathcal{W}}^d(T) = \mathrm{H}_{1,2}^{2,0}\left[\lambda\kappa_{\mathcal{W}} T^\delta\left|\begin{matrix}(1, \delta)\\ (0, 1), (1, \frac{\delta}{\nu})\end{matrix}\right.\right] \tag{16}$$

where $\kappa_{\mathcal{W}} = \frac{\tau\Gamma(1-\delta)\Gamma(1+\frac{\delta}{\nu})\gamma(2,\zeta\pi\theta^2)}{\zeta}$.

Proof: The result follows in the same line of (12) while applying [13, Eq. 2.3].

Remark 1: The Rayleigh fading is a special case of (9) and (14) when $m = 1$ and $\nu = 1$, respectively. When $m = 1$, applying [13, Eq. 1.60] to (9) and recognizing the fact that $\mathrm{G}_{2,2}^{1,1}\left[\frac{\Omega\xi}{T}\left|\begin{matrix}-1, 0\\ 0, -1\end{matrix}\right.\right] = \delta\left[\frac{T}{\xi\Omega} - 1\right]$ where $\delta[x]$ stands for the DiracDelta function, i.e., $\delta[x] = 0/; x \neq 0$, leads to

$$\mathbb{P}^x(T) = \exp\left(-T\frac{\sigma^2}{\Omega} - \mathcal{A}^x\left(\frac{T}{\Omega}, \delta\right)\right). \tag{17}$$

where $\mathcal{A}^x(\xi, \delta)$ is obtained form (10) by setting $m = 1$ and simplifying using ${}_{\mathrm{p}}\mathrm{F}_{\mathrm{q}}(\underline{a}_p; \underline{b}_{q-1}, a_p; z) = {}_{\mathrm{p-1}}\mathrm{F}_{\mathrm{q-1}}(\underline{a}_{p-1}; \underline{b}_{q-1}; z)$ as

$$\begin{cases}\mathcal{A}^d(\xi, \delta) = \frac{\tau\lambda\xi^\delta\Omega^\delta}{\zeta}\frac{\pi\gamma(2,\zeta\pi\theta^2)}{\delta\sin(\pi\delta)},\\ \mathcal{A}^c(\xi, \delta) = \frac{\delta^2\xi\Omega\ {}_3\mathrm{F}_2(1-\delta,1,1+\delta;2-\delta,2+\delta;-\xi\Omega)}{(\delta-1)(\delta+1)},\end{cases} \tag{18}$$

The same result could be obtained form (14) by setting $\nu = 1$ and simplifying using [13, Eq. 1.56].

The coverage formulas in (17) matches the well-known major result for Rayleigh fading obtained in [1, Eqs. 12, 15], validating once again the wider scope of our new analysis approach. Notice however that (17) constitutes a useful add on to [1, Eqs. 15] by deriving $\mathcal{A}^c(\xi, \delta)$ in closed-form.

Proposition 3 (generalized-$\mathcal{K}$ Fading): When h follows a generalized-$\mathcal{K}$ distribution with parameters (m, k, Ω) [6], then the D2D and cellular coverage is given by

$$\begin{aligned}\mathbb{P}_{\mathcal{K}}^x(T) \quad &= \quad \frac{\left(\frac{Tmk}{\Omega}\right)^m}{\Gamma(k)\Gamma(m)}\int_0^\infty \xi^{-m-1}e^{-\frac{Tmk}{\xi\Omega}} \\ &\quad \times \mathrm{U}\left(1-k, m-k+1; \frac{Tmk}{\xi\Omega}\right) \\ &\quad \times \exp\left(-\xi\sigma^2 - \mathcal{A}_{\mathcal{K}}^x(\xi, \delta)\right) d\xi,\end{aligned} \tag{19}$$

where $\mathrm{U}(a, b; z)$ stands for the Triconomi confluent hypergeometric function [12, Eq. (9.211.1)], and

$$\begin{cases}\mathcal{A}_{\mathcal{K}}^d(\xi, \delta) = \frac{\tau\lambda\xi^\delta\left(\frac{\Omega}{mk}\right)^\delta\Gamma(1-\delta)\Gamma(m+\delta)\Gamma(k+\delta)\gamma(2,\zeta\pi\theta^2)}{\zeta\Gamma(m)\Gamma(k)},\\ \mathcal{A}_{\mathcal{K}}^c(\xi, \delta) = \frac{\delta^2\mathrm{G}_{5,4}^{1,5}\left[\frac{\xi\Omega}{mk}\left|\begin{matrix}1+\delta, 1-k, 1-m, 1, 1-\delta\\ 1, 0, -\delta, \delta\end{matrix}\right.\right]}{\Gamma(m)\Gamma(k)}.\end{cases} \tag{20}$$

Proof: In 5G communications design, the combined effect of small-scale and shadowed fading needs to be properly addressed. Shadowing, which is due to obstacles in the local environment or human body (user equipments) movements, can impact link performance by causing fluctuations in the received signal. For instance, the shadowing effect comes to prominence in millimeter wave (mmWave) communications due to the higher carrier frequency. In this respect, the generalized-$\mathcal{K}$ ($\mathcal{GK}$) model was proposed by combining Nakagami-m multipath fading and Gamma-Gamma distributed shadowing [7]. The proof follows from (8) with $f_h(y) = \frac{(\sqrt{\frac{4km}{\Omega}})^{k+m}}{2^{k+m-1}\Gamma(m)\Gamma(k)} y^{\frac{k+m}{2}-1} K_{k-m}\left(\sqrt{2\frac{kmy}{\Omega}}\right)$ were $K_b(\cdot)$ is the Bessel function of the first kind of order b [12, Eq. (13.1.2)], and applying [13, Eqs. (2.3), (1.56)]. Moreover, resorting to the displacement theorem [11], it follows that $\mathcal{E}[h^j] = \frac{\Gamma(m+j)\Gamma(k+j)}{\Gamma(m)\Gamma(k)}\left(\frac{\Omega}{mk}\right)^j$ thereby yielding $\mathcal{A}^d_{\mathcal{K}}(\xi,\nu)$. The conversion method can incorporate an arbitrary fading distribution, but is not applicable when there is an exclusion zone in the interference field. Therefore $\mathcal{A}^c_{\mathcal{K}}(\xi,\delta)$ is obtained form (6) after substituting the hypergeometric function by its expression of Meijer's-G function [12, Eq. 9.304.8] and applying [12, Eq. 7.821.3].

Proposition 3 (shadowed κ-μ Fading): With overlay in-band D2D, the SINR CCDF of D2D and cellular links over shadowed κ-μ fading is

$$\mathbb{P}^x_{S\kappa\mu}(T) = \frac{\widetilde{\mathcal{C}}_{S\kappa\mu}}{T}\int_0^\infty G^{1,1,0,1,1}_{1,[1,1],0,[2,2]}\left[\begin{matrix}-\frac{\mu\kappa}{(\mu\kappa+m)} \\ \frac{\xi\Omega}{T\mu(1+\kappa)}\end{matrix}\middle|\begin{matrix}1+\mu \\ 1-m;0 \\ 0,1-\mu;0,-1\end{matrix}\right] \exp\left(-\xi\sigma^2 - \mathcal{A}^x_{S\kappa\mu}(\xi,\delta)\right)d\xi, \quad (21)$$

where $\widetilde{\mathcal{C}}_{S\kappa\mu} = \frac{\Omega}{\Gamma(m)\mu(1+\kappa)\left(\frac{\mu\kappa}{m}+1\right)^m}$, and $\mathrm{G}^{p,q,k,r,l}_{a,[c,e],b,[d,f]}(\cdot,\cdot)$ is the generalized Meijer's G-function of two variables [14]. Moreover in (21), $\mathcal{A}^x_{S\kappa\mu}(\xi,\nu)$ is obtained as

$$\begin{cases}\mathcal{A}^d_{S\kappa\mu}(\xi,\delta) = \frac{\tau\xi^\delta\Gamma(1-\delta)\gamma(2,\zeta\pi\theta^2)\Gamma(\mu+\delta)\,{}_2\mathrm{F}_1\left(\mu-m,\mu+\delta,\mu;-\frac{\mu\kappa}{m}\right)}{\zeta\left(\frac{\Omega}{\mu(1+\kappa)}\right)^{-\delta}\left(\frac{\mu\kappa}{m}+1\right)^{m-\mu-\delta}\Gamma(\mu)}; \\ \mathcal{A}^c_{S\kappa\mu}(\xi,\delta) = \frac{\delta^2\Omega\xi\sum_{k=1}^3\Theta_k\mathrm{F}_2\left(\mu+1,a_k,m;a_k+1,\mu;\frac{\mu\kappa}{\mu\kappa+m},-\frac{\xi\Omega}{\mu(1+\kappa)}\right)}{(1+\kappa)(\delta-1)(\delta+1)\left(\frac{\mu\kappa}{m}+1\right)^m},\end{cases} \quad (22)$$

where $\Theta_k = \prod_{j=1,j\neq k}^3 \frac{a_j}{a_j-a_k}$ with $a_k \in \{1, 1-\delta, 1+\delta\}, k = 1,\ldots,3$, and F_2 stands for Appell's function [17, Eq. 27].

Proof: See Appendix B.

Corollary 3: In interference-limited κ-μ shadowed environment, the coverage of D2D communication is obtained as

$$\mathbb{P}^d_{S\kappa\mu}(T) = \frac{\widetilde{\mathcal{C}}_{S\kappa\mu}}{\delta T\kappa^{\frac{1}{\delta}}_{S\kappa\mu}} H^{1,1,0,1,2}_{1,[1,1],0,[2,2]} \left[\begin{matrix}-\frac{\mu\kappa}{(\mu\kappa+m)} \\ \frac{\lambda\kappa^{\frac{-1}{\delta}}_{S\kappa\mu}}{T\mu(1+\kappa)}\end{matrix}\middle|\begin{matrix}(1+\mu,1) \\ (1-m,1);(1-\frac{1}{\delta},\frac{1}{\delta});(0,1) \\ (0,1),(1-\mu,1);(0,1),(-1,1)\end{matrix}\right], \quad (23)$$

where $\kappa_{S\kappa\mu} = \frac{\tau\Gamma(1-\delta)\Gamma(\mu+\delta)\,{}_2\mathrm{F}_1\left(\mu-m,\mu+\delta,\mu;-\frac{\mu\kappa}{m}\right)\gamma(2,\zeta\pi\theta^2)}{\zeta\left(\frac{\mu\kappa}{m}+1\right)^{m-\mu-\delta}\Gamma(\mu)}$, and $H[\cdot,\cdot]$ denotes the Fox-H function (FHF) of two variables [16, Eq.(1.1)] also known as the bivariate FHF.

Proof: When $\sigma^2 \to 0$, $\mathbb{P}^x_{S\kappa\mu}(T)$ in (21) becomes

$$\mathbb{P}^d_{S\kappa\mu}(T) = \frac{\widetilde{\mathcal{C}}_{S\kappa\mu}}{T}\int_0^\infty G^{1,1,0,1,1}_{1,[1,1],0,[2,2]}\left[\begin{matrix}-\frac{\mu\kappa}{(\mu\kappa+m)} \\ \frac{\xi\Omega}{T\mu(1+\kappa)}\end{matrix}\middle|\begin{matrix}1+\mu \\ 1-m;0 \\ 0,1-\mu;0,-1\end{matrix}\right] \mathrm{H}^{1,0}_{0,1}\left[\mathcal{A}^d_{S\kappa\mu}(\xi,\delta)\middle|\begin{matrix}- \\ (0,1)\end{matrix}\right]d\xi. \quad (24)$$

Then applying [13, Eq. 2.11] yields the desired result after some algebraic manipulations.

Remark 2: The κ-μ shadowed distribution is a very flexible model which contains as special cases the majority of the linear fading models proposed in the open literature, including Rayleigh, Rice (Nakagami-n), Nakagami-m, Hoyt (Nakagami-q), One-Sided Gaussian, κ-μ, η-μ and Rician shadowed to name a few [5, Table 1]. These fading models are unlikely tractable form (21) and (23) due to the high degree of difficulty in handling the Meijer's-G and Fox's-H functions of two variables.

IV. NUMERICAL AND SIMULATION RESULTS

In the following, we compare numerical results for different fading models with the following parameters: macro BS intensity $\lambda_c = \frac{1}{\pi 500^2}$, D2D user intensity $\lambda = 10\lambda_c$, ALOHA transmit probability $\tau = 0.8$, path-loss exponent $\alpha = 4$, and mode selection threshold $\theta = 200$m Without loss of generality, we assume identical fading parameters across the intended and interference link.

Fig. 1 and Fig. 2 show the SINR CCDF of the D2D overlaid network for different fading environments. As expected, the performance deteriorates as the shadowing becomes more pronounced or the fading severity parameter m becomes smaller. The D2D links have a closer transmission range than cellular links, which leads to a higher SINR distribution for D2D links than cellular links.

Fig. 3 depicts the D2D SIR CCDF in Weibull and Nakagami-m fading channels. As expected, the coverage probability deteriorates by decreasing m or ν. The coverage increment of D2D link in Weibull fading is notable over the whole range of ν, whereas the increment of D2D coverage in Nakagami-m fading is barely distinguishable after Rayleigh.

V. CONCLUSION

We have presented a unified method to computing the D2D SINR distribution of an arbitrary fading model. Remarkably, the paper embodies the H-transform theory into a unifying coverage analysis framework for D2D-commendation-enabled cellular networks, leading to new SINR expressions for the most versatile fading distributions. By virtue of some H-transform asymptotic expansions, the high signal-to-interference-plus-noise ratio

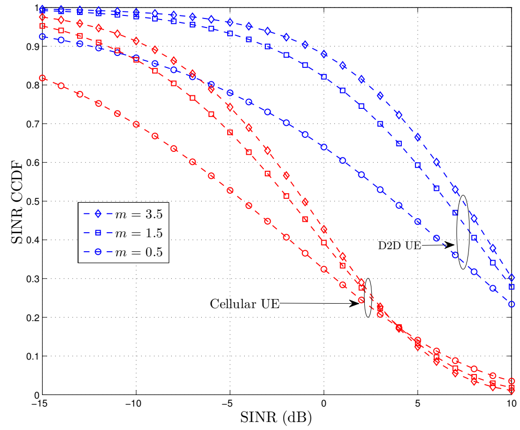

Fig. 1. SINR CCDF P_m^x in Nakagami-m fading.

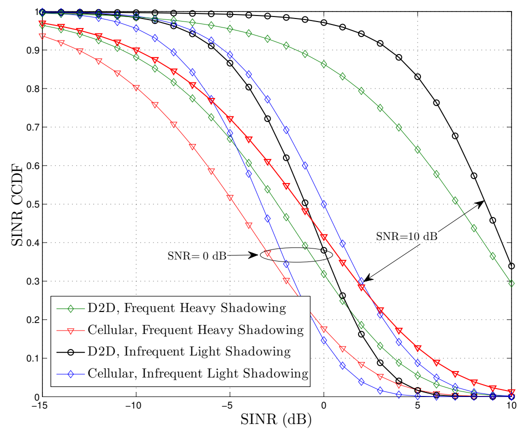

Fig. 2. SINR CCDF $P_{\mathcal{K}}^x$ in infrequent light shadowing ($k = 75.1155$) and frequent heavy shadowing ($k = 1.0931$) environments with $m = 2.5$.

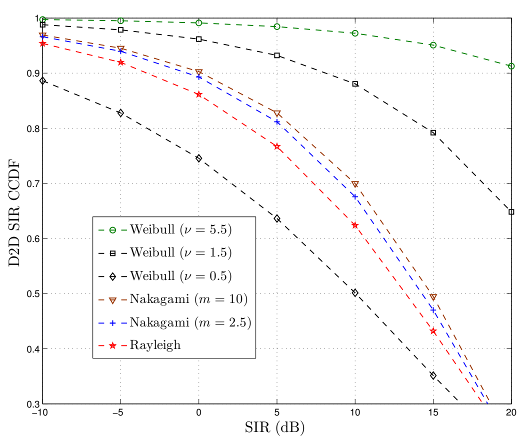

Fig. 3. D2D SIR coverage probability.

(SINR) analysis culminates in easy-to-compute expressions of the coverage probability.

VI. Appendix

A. Proof of Theorem 1:

The SINR CCDF $\mathbb{P}^x(T)$ may be retrieved from its Laplace transform as

$$\mathcal{L}_{\mathbb{P}^x}(z) = \frac{1}{z} - \frac{M_{\text{SINR}}^x(z)}{z}, \quad z \in \mathbb{R}_+, \tag{25}$$

where $M_{\text{SINR}}^x(z)$ denotes the SINR moment generating function recently obtained in [2, Theorem 1] as

$$\begin{aligned} M_{\text{SINR}}^x(s) &= 1-2\sqrt{s}\int_0^\infty \mathcal{E}_h\left[\sqrt{h}\mathrm{J}_1\left(2\sqrt{sh}\xi\right)\right] \\ &\quad e^{-\sigma^2\xi^2}\mathcal{L}_{\mathcal{I}_x}(\xi^2)d\xi, \end{aligned} \tag{26}$$

where $\mathrm{J}_1(\cdot)$ is the Bessel function of the second kind and first order [12, Eq. 8.402] and $\mathcal{L}_{\mathcal{I}_\S}(s) = \mathcal{E}\left[e^{-sI}\right]$ denotes the Laplace transform of the aggregate interference at a typical D2D for $x = d$ and at a typical cellular user for $x = c$. Substituting (26) into (25), yields

$$\begin{aligned} \mathbb{P}^x(T) &\stackrel{(a)}{=} 2\int_0^\infty \mathcal{E}_h\left[\sqrt{h}\ \mathcal{L}^{-1}\left(\frac{\mathrm{J}_1\left(2\sqrt{sh}\xi\right)}{\sqrt{s}}, T\right)\right] \\ &\quad e^{-\sigma^2\xi^2}\mathcal{L}_{\mathcal{I}_x}(\xi^2)d\xi, \end{aligned} \tag{27}$$

whereby

$$\begin{aligned} \mathcal{L}^{-1}\left(\frac{\mathrm{J}_1\left(2\sqrt{sh}\xi\right)}{\sqrt{s}}, T\right) &\stackrel{(a)}{=} \xi\sqrt{h} \\ &\quad \mathcal{L}^{-1}\left(\mathrm{H}_{0,2}^{1,0}\left[sh\xi^2\middle|\begin{matrix} - \\ (0,1),(-1,1)\end{matrix}\right], T\right) \\ &\stackrel{(b)}{=} \frac{\xi\sqrt{h}}{T}\mathrm{H}_{1,2}^{1,0}\left[\frac{h\xi^2}{T}\middle|\begin{matrix}(0,1) \\ (0,1),(-1,1)\end{matrix}\right], \end{aligned} \tag{28}$$

where (a) and (b) follows form applying [13, Eq. 1.127] and [13, Eq. 2.21], respectively. Plugging (28) into (27) and carrying out the change of variable $x = \xi^2$ yield

$$\begin{aligned} \mathbb{P}^x(T) &= \frac{1}{T}\int_0^\infty \mathcal{E}_h\left[h\ \mathrm{H}_{1,2}^{1,0}\left[\frac{h\xi}{T}\middle|\begin{matrix}(0,1) \\ (0,1),(-1,1)\end{matrix}\right]\right] \\ &\quad e^{-\sigma^2\xi}\mathcal{L}_{\mathcal{I}_x}(\xi)d\xi. \end{aligned} \tag{29}$$

For overlay D2D, the Laplace transform of the interference at the cellular BS whose macrocell coverage region is approximated by a disk $\mathcal{U} = \mathcal{B}(0, R)$ with $R = 1/\sqrt{\pi\lambda_c}$ is given by

$$\begin{aligned} \mathcal{L}_{\mathcal{I}_c}(\xi) &= \mathcal{E}_{\Psi,h}\left[\exp\left(-\xi\sum_{i\in\widetilde{\Psi}_c\bigcap\mathcal{U}^c} P_{i,c}h_{i,c}L_{i,c}^{-\alpha}\right)\right] \\ &\stackrel{(a)}{=} e^{-2\pi\lambda_c\mathcal{E}_{h,P_c}\left[\int_R^\infty\left(1-\exp\left(-\xi P_c h v^{-\alpha}\right)\right)v dv\right]} \\ &\stackrel{(b)}{=} e^{-2\pi\lambda_c\mathcal{E}_{h,P_c}\left[hP_c\xi\int_R^\infty \frac{e^{-\xi P_c h v^{-\alpha}}{}_1\mathrm{F}_1\left(1,2,\xi P_c h v^{-\alpha}\right)dv}{v^{\alpha-1}}\right]} \\ &\stackrel{(c)}{=} e^{-\frac{2R^{-\alpha}\xi\mathcal{E}_{h,P_c}\left[hP_c\,{}_2\mathrm{F}_2\left(1,\frac{2}{\alpha}+1;2;\frac{2}{\alpha}+2;-\xi P_c h\right)\right]}{R^\alpha\alpha\left(1-\frac{2}{\alpha}\right)}}, \end{aligned} \tag{30}$$

where we have used the probability generating functional of PPP in (a), and $(1-e^{-x})/x = e^{-x}{}_1\mathrm{F}_1(1,2;x)$ in (b). Finally (c) follows from letting $t = x^{-\alpha}$ and applying $\int x^{\beta-1}e^{-cx}{}_1\mathrm{F}_1(a,b,cx) = \frac{x^\beta}{\beta}{}_2\mathrm{F}_2(b-a,\beta,b,\beta+1,-cx)$.

For overlay D2D, the Laplace transform of the interference at the D2D receiver $\mathcal{L}_{\mathcal{I}_d}(\xi)$ follows from [9, Eq.22] as

$$\mathcal{L}_{\mathcal{I}_d}(\xi) = \exp\left(-\pi\tau\lambda_d\xi^\delta\Gamma(1-\delta)\,\mathcal{E}[P_d^\delta]\mathcal{E}[h^\delta]\right), \quad (31)$$

Substituting (30) and (31) into (29) leads to Theorem 1 after recognizing that $\mathrm{H}_{1,2}^{1,0}\left[\frac{h\xi}{T}\middle|\begin{matrix}(0,1)\\(0,1),(-1,1)\end{matrix}\right] = \mathrm{G}_{1,2}^{1,0}\left[\frac{h\xi}{T}\middle|\begin{matrix}0\\0,-1\end{matrix}\right]$.

B. Proof of Proposition 3:

The shadowed κ-μ distribution is used to account for small scale fading which originates due to LOS or NLOS conditions, whence its extreme versatility including as special cases nearly all linear fading models adopted in the open literature [5, Table I]. In this model, the dominant signal components (DSCs) are subject to Nakagami-m shadowing. The probability density function (PDF) of $h \sim S_{\kappa,\mu,m}(\Omega;\kappa,\mu,m)$ is

$$f_{h,S\kappa-\mu}(y) = \frac{\mu^\mu m^m(1+\kappa)^\mu}{\Gamma(\mu)\Omega^\mu(\mu\kappa+m)^m}\left(\frac{y}{\Omega}\right)^{\mu-1}e^{-\frac{\mu(1+\kappa)}{\Omega}y}\;{}_1\mathrm{F}_1\left(m,\nu,\frac{\mu^2\kappa(1+\kappa)}{\Omega(\mu\kappa+m)}y\right), \quad (32)$$

where $\Omega = \mathcal{E}[h]$, κ, μ, and m, are positive real shape parameters, and ${}_1\mathrm{F}_1(\cdot)$ denotes the confluent hypergeometric function of [12, Eq. (13.1.2)]. Then it follows that

$$\begin{aligned}\Phi(\xi,T) &\overset{(a)}{=} \frac{\mathcal{C}_{S\kappa\mu}\Gamma(\mu)}{\Gamma(m)}\int_0^\infty x^\mu e^{-\frac{\mu(1+\kappa)x}{\Omega}}\mathrm{H}_{1,2}^{1,0}\left[\frac{\xi x}{T}\middle|\begin{matrix}(0,1)\\(0,1),(-1,1)\end{matrix}\right]\\ &\qquad \mathrm{H}_{1,2}^{1,1}\left[-\frac{\mu^2\kappa(1+\kappa)x}{\Omega(\mu\kappa+m)}\middle|\begin{matrix}(1-m,1)\\(0,1),(1-\mu,1)\end{matrix}\right]dx\\ &\overset{(b)}{=} \frac{\mathcal{C}_{S\kappa\mu}\Gamma(\mu)}{\Gamma(m)}\left(\frac{\mu(1+\kappa)}{\Omega}\right)^{-\mu-1}\\ &\mathrm{H}_{1,[1,1],0,[2,2]}^{1,1,0,1,1}\left[\begin{matrix}-\frac{\mu\kappa}{(\mu\kappa+m)}\\ \frac{\xi\Omega}{T\mu(1+\kappa)}\end{matrix}\middle|\begin{matrix}(1+\mu,1)\\(1-m,1);(0,1)\\(0,1),(1-\mu,1);(0,1),(-1,1)\end{matrix}\right] \quad (33)\end{aligned}$$

where $\mathcal{C}_{S\kappa\mu} = \frac{\mu^\mu m^m(1+\kappa)^\mu}{\Gamma(\mu)\Omega^\mu(\mu\kappa+m)^m}$ and (a) follows from exploiting the equality ${}_1\mathrm{F}_1(a,b;z) = \frac{\Gamma(b)}{\Gamma(a)}\mathrm{H}_{1,2}^{1,1}\left[-z\middle|\begin{matrix}(1-a,1)\\(0,1),(1-b,1)\end{matrix}\right]$ [13, A.6]. The Laplace transform of the product of two Fox-H functions functions [13, Eq. 2.6.2] was applied to reach (b). The function $\mathrm{H}_{1,2}^{1,1}[\cdot,\cdot]$ denotes the generalized Fox's H-function of two variables and it reduces to the generalized Meijer's G-function of two variables with the help of [13, Eq. 2.3.1] as shown in (21). Recalling that under shadowed κ-μ fading

$$\mathcal{E}[h^j] = \frac{\left(\frac{\Omega}{\mu(1+\kappa)}\right)^j\Gamma(\mu+j)}{\left(\frac{\mu\kappa}{m}+1\right)^{m-\mu-j}\Gamma(\mu)}{}_2\mathrm{F}_1\left(\mu-m,\mu+j,\mu;-\frac{\mu\kappa}{m}\right)$$

[9, Eq.10] thereby yielding $\mathcal{A}_{\mathcal{K}}^d(\xi,\alpha)$ as in (22). In the other hand $\mathcal{A}_{\mathcal{K}}^c(\xi,\alpha)$ is obtained from (6) after resorting to ${}_3\mathrm{F}_3(1-\delta,1,1+\delta;2-\delta,2,2+\delta;-\xi h) = \sum_{k=1}^3 {}_1\mathrm{F}_1(a_k,a_k+1;-\xi h)\prod_{j=1,j\neq k}^3\frac{a_j}{a_j-a_k}$ where $a_k \in \{1,1-\delta,1+\delta\}, k = 1,\ldots,3$ and applying [17, Eq. 27], thereby yielding

$$\mathrm{F}_2\left(a,b,b',c,c';\frac{w}{p},\frac{z}{p}\right) = \frac{p^a}{\Gamma(a)}\int_0^\infty x^{a-1}e^{-px}{}_1\mathrm{F}_1(b,c,wx)\;{}_1\mathrm{F}_1(b',c',xz)\,dx. \quad (34)$$

References

[1] X. Lin, J. G. Andrews, and A. Ghosh, "Spectrum Sharing for Device-to-Device Communication in Cellular Networks," *IEEE Trans. Wirel. Commun.,* vol. 13, no. 12, pp. 1-31, Dec. 2014.

[2] I. Trigui, S. Affes, and B. Liang, "Unified Stochastic Geometry Modeling and Analysis of Cellular Networks in LOS/NLOS and Shadowed Fading" CoRR, vol. arXiv:1609.09389, 2016. [Online].

[3] M. D. Yacoub, "The κ-μ distribution and the η-μ distribution," *IEEE Antennas Propag. Mag.,* vol. 49, no. 1, pp. 68-81, Feb. 2007.

[4] N. Beaulieu and X. Jiandong, "A novel fading model for channels with multiple dominant specular components," *IEEE Wireless Commun. Lett.,* vol. 4, no. 1, pp. 54-57, Feb. 2015.

[5] J. F. Paris, "Statistical Characterization of κ-μ Shadowed Fading," *IEEE Trans. Veh. Technol.,* vol.63, no. 2, pp. 518-526, Feb. 2014.

[6] M. K. Simon and M.-S. Alouini, *Digital Communication over Fading Channels*. Wiley-Interscience, 2005, vol. 95.

[7] I. Trigui, S. Affes, and and A. Stephenne, "Performance analysis of mobile radio systems over composite fading/shadowing channels with co-located interference", *IEEE Trans. Wirel. Commun.,* vol. 8, no. 7, Jul. 2009

[8] M. Peng, Y. Li, T. Q. S. Quek, and C. Wang, "Device-to-Device Underlaid Cellular Networks under Rician Fading Channels," *IEEE Trans. Wirel. Commun.*, vol. 13, no. 8, pp. 42474259, Aug. 2014

[9] Y. J. Chun, S. L. Cotton, H. S. Dhillon, F. J. Lopez-Martinez, J. F. Paris, and S. Ki Yoo "A Comprehensive Analysis of 5G Heterogeneous Cellular Systems operating over κ-μ Shadowed Fading Channels", CoRR, vol. arXiv:1609.09389, 2016. [Online].

[10] S. Parthasarathy and R. K. Ganti, "SIR distribution in downlink Poisson point cellular network with κ-μ shadowed fading," may 2016. [Online]. Available: http://arxiv.org/abs/1605.03763.

[11] H. S. Dhillon and J. G. Andrews, "Downlink rate distribution in heterogeneous cellular networks under generalized cell selection," *IEEE Wirel. Commun. Lett.*, vol. 3, no. 1, pp. 4245, 2014.

[12] I. S. Gradshteyn and I. M. Ryzhik, *Table of Integrals, Series and Products,* 5th ed., Academic Publisher, 1994.

[13] A. M. Mathai and R. K. Saxena, *The H-Function With Applications in Statistics and Other Disciplines.* New Delhi, India: Wiley Eastern, 1978.

[14] R. U. Verma, "On some integrals involving Meijer's G-fucntion of two variables", *Proc. Nat. Inst. Sci. India*, vol. 39, Jan. 1966.

[15] L. H. Afify, H. ElSawy, T. Y. Al-Naffouri, and M.-S. Alouini, "The influence of Gaussian signaling approximation on error performance in cellular networks," *IEEE Commun. Lett.,* vol. 19, no. 12, Dec. 2015.

[16] P. Mittal and K. Gupta, "An integral involving generalized function of two variables", *Proc. Ind. Acad. Sci.*, vol. 75, no. 3, pp. 117123, 1972.

[17] Yu.A. Brychkova and N. Saad , "On some formulas for the Appell function $\mathrm{F}_2(a,b,b';c,c;w;z)$ *Integral Transforms and Special Functions,* vol. 25, no. 2, pp. 111-123, 2014.